

On the role of preferential segregation in flame dynamics in polydisperse evaporating sprays

By L. Fréret[†], O. Thomine[‡], J. Réveillon[‡],
S. de Chaisemartin[¶], F. Laurent^{||} AND M. Massot^{||}

The use of robust and accurate Eulerian/Eulerian formulations in the modeling of reactive two-phase flow would be a major step forward in the framework of turbulent combustion modeling with massively parallel supercomputers. Therefore, the ability of the Eulerian multi-fluid model to capture all stages of turbulent spray combustion has been tested and compared with a usual Lagrangian formulation. The multi-fluid model and related dedicated schemes and algorithms are able to characterize properly the spray dispersion and segregation as well as the vaporization dynamics leading to the fuel mass fraction topology. Eventually, flame propagation and structure in 2D and 3D forced isotropic homogeneous turbulence have been characterized showing the capacity of the multi-fluid model to simulate such reactive flows with results with the same level of accuracy as a baseline solution obtained with Lagrangian droplet tracking.

1. Introduction

Spray combustion modeling is a fundamental stage in the design of combustion chambers that relies on accurate computational tools to rapidly design and develop high efficiency, low emission engines. However, there are numerous physical and numerical difficulties because of the presence of many different time and space characteristic scales when liquid and gas are mixing. Thus, two-phase flow models need many developments and improvements to characterize correctly complex industrial flows in CFD solvers. In such configurations, the gas, which is a continuum, is best represented by a Eulerian description. However, in the framework of dispersed flows, particles or droplets can be modeled either by a Lagrangian or a Eulerian description (Gouesbet & Berlemont 1998). Both these descriptions are now well established and they have proven their efficiency in very separate domains of multi-phase flow simulations. Lagrangian methods combine an efficient modeling of the polydisperse phase, a high numerical efficiency, and an easiness of implementation. Nevertheless, in the framework of domain decomposition for parallel computations, it requires the use of complex and costly dynamic partitioning methods, to ensure a good load balancing between the different parallel processes (see Garcia 2009). Hence, Eulerian methods provide an interesting alternative to Lagrangian methods, since they can easily take advantage of massively parallel computations, but require special attention in terms of mathematical structure and numerical diffusion.

The objective of this work is to carry out the first exhaustive comparisons between

[†] Laboratoire d'Imagerie Paramétrique, 15 rue de l'école de médecine, 75006 Paris, France

[‡] CORIA, UMR CNRS 6614 Université and INSA de Rouen, Avenue de l'université, 76800 St Étienne du Rouvray, France

[¶] IFP Energies nouvelles, 1-4 avenue de Bois-Préau, 92852 Reuil-Malmaison, France

^{||} Laboratoire EM2C - UPR CNRS 288, Ecole Centrale Paris, Grande voie des vignes, 92295 Chatenay Malabry, France

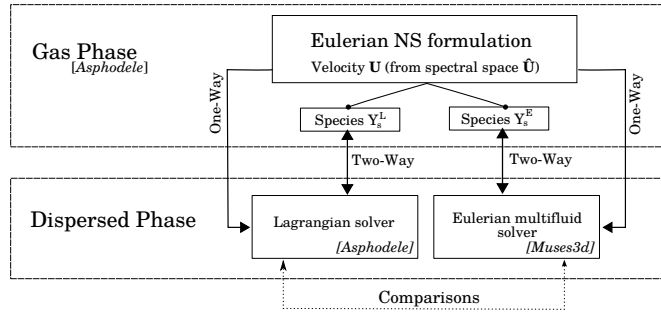


FIGURE 1. Sketch of the coupling between Eulerian and Lagrangian codes. *Muses3d* is a Eulerian solver for the dispersed phase while *Asphodele* is a Lagrangian solver for the dispersed phase and a Eulerian solver for the gas phase.

Eulerian-Lagrangian (EL) and Eulerian-Eulerian (EE) formulations of a reactive two-phase flow in a partially premixed regime. To discriminate as much as possible the various physical interactions between the flow, the spray and the flame, a straightforward and controllable configuration has been selected: a forced homogenous turbulence whose main characteristics are that kinetic energy and integral length scale are prescribed (Guichard *et al.* 2004) and that they remain statistically stationary during the whole computation through a spectral forcing. In this study, we will restrict ourselves to a constant-density gaseous flow field for three reasons. First, the spectral forcing requires a spectral resolution of the Navier-Stokes equations written in a constant-density context. Second, by doing so we couple a single gaseous flow field to the two dispersed phase solvers; accordingly, all the characteristics of the turbulence may be considered to be known and we can evaluate and compare the impact of the turbulence on spray dispersion, vapor mixing and combustion. Third, constant-density combustion is generally assumed in theoretical studies to suppress the impact of the heat release effects on the velocity field. The central idea is to resolve an Arrhenius law based on the burnt gases mass fraction instead of the temperature. Several analytical works on polydisperse spray flame propagation and stability have been carried out with this hypothesis (see Greenberg *et al.* 2001 and references therein). Even if the heat release can not be considered as negligible, as shown in Costa 2000, the restriction to constant-density flows still preserves many properties linked to the propagation of a flame front and the present paper is mainly aimed at comparing the two Eulerian-Lagrangian (EL) and Eulerian-Eulerian (EE) descriptions in the presence of a propagating front.

2. Two-phase flow simulations

2.1. Gas and disperse phase models and numerical methods

Various sets of governing equations are coupled together to carry out simulations thanks to the association of two codes: *Asphodele* from CORIA (Gas phase + Lagrangian spray solver) and *Muses3d* from EM2C (Eulerian multi-fluid solver). A sketch of the coupling used in this work is presented in Fig 1. A first system of Eulerian conservation equations solves the gas phase evolution, a second system of Eulerian multi-fluid conservation equations allows to resolve the spray evolution while a third set of ODEs corresponds to the Lagrangian description of a spray evolution. Simultaneous simulations using a single gaseous phase evolution lead to very accurate and detailed comparisons of the spray dynamics and evaporation through EL and EE models.

Because of the forcing procedure restrictions, the gas phase velocity is evaluated in the spectral space through the following equation:

$$\frac{\partial \hat{\mathbf{u}}}{\partial t} = \hat{\mathbf{a}} + \frac{f_\kappa}{\tau_f} \hat{\mathbf{u}} \quad , \quad (2.1)$$

where $\hat{\mathbf{a}}$ represents the Navier-Stokes contributions for an incompressible flow (Lesieur 2007). The forcing function f_κ , detailed in Guichard *et al.* 2004, is real and depends on both time t and wave number magnitude κ . The principle of the model is to relax the simulated spectrum towards a model spectrum for a given range of low wave numbers.

The evolution of the air/vapor mixture is described in physical space so that it can be easily coupled with both Lagrangian and Eulerian descriptions of the evaporating spray. The following relation applies for any species s , which stands for either the fuel (f), the oxidizer (o) or the burnt gases (b):

$$\frac{\partial Y_s^\alpha}{\partial t} + \frac{\partial Y_s^\alpha u_i}{\partial x_i} = D \frac{\partial^2 Y_s^\alpha}{\partial x_i^2} + \dot{\omega}_s^\alpha + \delta(s-f) \dot{d}_f^\alpha + \dot{\epsilon}_s^\alpha \quad , \quad (2.2)$$

where D is the species common diffusion coefficient and the velocity components u_i are obtained from an inverse Fourier transform of the spectral velocity field: $u_i = FT^{-1}(\hat{u}_i)$. Two strictly independent sets of species equations are solved: Y_s^L that are coupled with the Lagrangian description of the spray and, on the other hand, Y_s^E that are coupled with the Eulerian multi-fluid solver (see Fig 1). Only the velocity field evolution is common to both the mass fraction sets. The reaction rate of the considered species is denoted by $\dot{\omega}_s^\alpha$. It is obtained using a single step Arrhenius law describing the one-step kinetics $f + \nu o = (1 + \nu)b$, with $\nu = 15$ in our configuration, close to n-heptane stoichiometric ratio. Since a constant density approach is applied, temperature is constant in the domain. Thus, an artificial temperature T_a^α given by $T_a^\alpha = T_0(1 + 4Y_b^\alpha)$ based on the burnt gases mass fraction Y_b^α has been used, T_0 being the fresh gases initial temperature. Coupling the two dispersed phase solvers (Lagrangian and Eulerian) is realized through the mass source term \dot{d}_f^L and \dot{d}_f^E , respectively. An artificial correction coefficient, $\dot{\epsilon}_s^\alpha$, ensures a constant density flow by withdrawing a part of the gaseous mixture proportional to the local mass fraction $\dot{\epsilon}_s^\alpha = -Y_s^\alpha \dot{d}_f^\alpha$. Mass fraction equations are solved with a third order Runge-Kutta scheme, which is also used for the spectral space momentum resolution. Similar subtime-steps are applied for both spectral and physical solvers. A fourth order finite difference scheme allows to determine the spatial derivatives. As for the spectral velocity field, periodic boundary conditions have been used.

As mentioned in the introduction, a discrete Lagrangian approach is adopted to follow the spray evolution within the gaseous oxidizer. By denoting a_k , \mathbf{v}_k and \mathbf{x}_k the diameter, the velocity and position vectors of every droplet k , respectively, the following relations:

$$\frac{d\mathbf{x}_k}{dt} = \mathbf{v}_k, \quad (2.3) \quad \frac{d\mathbf{v}_k}{dt} = \frac{(\mathbf{u}(\mathbf{x}_k, t) - \mathbf{v}_k)}{\beta_k^{(v)}}, \quad (2.4) \quad \frac{da_k^2}{dt} = -\frac{a_k^2}{\beta_k^{(a)}}, \quad (2.5)$$

are used to track the droplets throughout the computational domain. The vector \mathbf{u} represents the gas velocity at the droplet position \mathbf{x}_k . The right hand side term of equation (2.4) stands for a drag force applied to the droplet where $\beta_k^{(v)}$ is a dynamic relaxation time $\beta_k^{(v)} = \tau_p a_k^2 / a_0^2$. The diameter of the droplet k is a_k and a_0 is the initial diameter of any droplet of the initially monodisperse spray. The initial characteristic kinetic time of the considered droplets is denoted by τ_p . The unitary stoichiometric ratio leads to a global mass ratio of fuel inferior to 10% and a constant pressure configuration is con-

sidered. In such a configuration, the saturation level determining the evaporation rate depends mainly on the temperature level surrounding the droplet. To correlate the spray evaporation with the flame propagation, the artificial temperature T_a^α has been utilized through the following expression of the mass transfer number

$$B = \frac{T_a^L - T_0}{T_b - T_0} \left(\exp \left(\frac{A a_0^2}{\tau_v} \right) - 1 \right), \quad (2.6)$$

where A is a constant depending on liquid and gas properties (Reveillon & Demoulin 2007) and $T_b = T_a(Y_b = 1)$ the burnt gases' temperature. B is introduced in the expression of the evaporation rate through the evaporation time $\beta_k^{(a)}$ defined by $\beta_k^{(a)} = A a_k^2 / \ln(1 + B)$. The coupling term $\dot{d}_f^{L(n)}$ affects the mixture fraction evolution owing to a distribution of the Lagrangian mass on the n^{th} node of the Eulerian grid. One may write $\dot{d}_f^{L(n)} = -\rho_d \frac{\pi}{4} \frac{1}{V} \sum_k \alpha_k^{(n)} a_k^3 / \beta_k^{(a)}$, where $\alpha_k^{(n)}$ is the distribution coefficient of the k^{th} droplet source term on the n^{th} node. Considering all the nodes affected by the k^{th} droplet, it is necessary to have $\sum_n \alpha_k^{(n)} = 1$ to conserve mass during the EL coupling. The values of $\alpha_k^{(n)}$ are chosen as the regressive normalized distances between the droplets and all surrounding nodes.

Another approach is to consider a Eulerian description of the spray, using the multi-fluid method developed by Laurent & Massot (2001) and Massot (2009). This method has been successfully used for small and moderate Stokes numbers (for example see Kah *et al.* 2010; de Chaisemartin 2009 for detailed comparisons with a Lagrangian description in case of axisymmetrical polydisperse free jets in a perturbed gaseous field; Fréret *et al.* 2010 for a three-dimensional non-evaporating spray dispersion comparison between these two numerical descriptions). The Eulerian multi-fluid method (EMM) is derived from a kinetic level of description based on the monokinetic velocity distribution assumption. The droplet size phase space is discretized into sections and a system of conservation laws over each fixed size interval $[S_k, S_{k+1}[$ is solved:

$$\begin{cases} \partial_t m^k + \partial_{\mathbf{x}} \cdot (m^k \bar{\mathbf{v}}^k) = -(E_1^{(k)} + E_2^{(k)}) m^k + E_1^{(k+1)} m^{(k+1)}, \\ \partial_t (m^k \bar{\mathbf{v}}^k) + \partial_{\mathbf{x}} \cdot (m^k \bar{\mathbf{v}}^k \otimes \bar{\mathbf{v}}^k) = -(E_1^{(k)} + E_2^{(k)}) m^k \bar{\mathbf{v}}^k + E_1^{(k)} m^{(k+1)} \bar{\mathbf{v}}^{(k+1)} + m^k \bar{\mathbf{F}}^k, \end{cases}$$

where m^k is the mass concentration of droplets, $\bar{\mathbf{v}}^k$ is the average velocity in the k^{th} section, $E_1^{(k)}$ are exchange terms between successive sections and $E_2^{(k)}$ are exchange terms with the gaseous phase. The average external force is $\bar{\mathbf{F}}^k$. The mass coupling with the carrier phase is done through $\dot{d}_f^E = \sum_{k=1}^{N_S} m^k E_2^{(k)}$, where N_S is the total number of sections. A Strang splitting algorithm separates transport in physical space from the evolution in phase space. The numerical schemes involve a very low level of numerical diffusion and are able to deal with singularities and stiffness (de Chaisemartin 2009).

2.2. DNS Configuration and parallel capability

In a preliminary stage, the turbulent gaseous phase evolves so that the statistical properties reach a steady state thanks to the FC-DFS forcing procedure (Guichard *et al.* 2004) that keeps the mean kinetic energy at the prescribed level. All characteristic values of the turbulence and reference parameters are to be found in Reveillon & Demoulin 2007. During this preliminary stage, monodisperse non-evaporating particles are randomly embedded throughout the computational domain with a zero initial velocity and the drag force sets particles in motion. Turbulence properties being fixed, simulations are carried

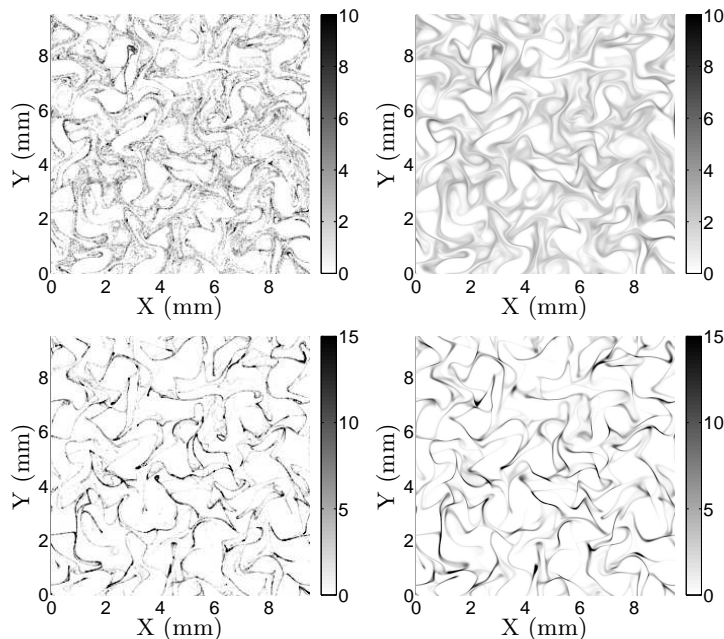


FIGURE 2. Droplet number density obtained from the Lagrangian (left) and Eulerian (right) simulations for $St = 0.2$ (top) and $St = 1$ (bottom) at $t = 0$, a reference time set after several eddy turnover times when droplets and gas have reached a dynamical equilibrium.

out with prescribed τ_p parameter. Two Stokes numbers $St = \tau_p/\tau_\kappa$ based on the Kolmogorov time scale τ_κ were considered in this study: $St = 0.2$ and $St = 1$. In our 2D configuration, the grid mesh used in *Asphodele* is 256^2 and the one used in *Muses3d* is 600^2 , whereas in 3D, we use 128^3 for both. Ten sections are used to describe the evaporation process within the multi-fluid model. The two codes have been optimized on parallel architecture, and the Eulerian solver *Muses3d* reaches an efficiency of one up to 512 cores on the Certainty cluster of the Center for Turbulence Research.

3. Results and discussion

The objective is to carry out qualitative but also quantitative comparisons between both Lagrangian and Eulerian formulations. Because of its intrinsic properties, the results from the Lagrangian solver are considered as a reference. The assessment of the Eulerian multi-fluid solver follows three axes: (i) the capture of the spray dispersion and segregation, (ii) a correct evaluation of the fuel vapor topology and (iii) the characterization of the flame properties and structure.

3.1. Spray dispersion and segregation

The Eulerian multi-fluid description of the spray dynamics are presented in this section for two Stokes numbers, based on the Kolmogorov time scale: $St = 0.2$, corresponding to light droplets still undergoing smallscale mixing (see figure 2 (top)) and $St = 1$, corresponding to heavier droplets being submitted to a strong segregation, since they are not affected by smallscale velocity variations, but at the same time, with limited crossing trajectories so that the Eulerian model remains relevant (see figure 2 (bottom)). In this

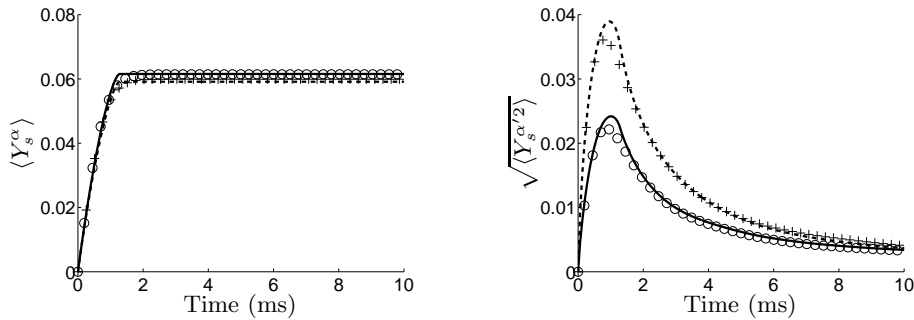


FIGURE 3. Time evolution of the mean (left) and rms (right) of the fuel vapor mass fraction from the Eulerian (Y_f^E - symbol) and Lagrangian (Y_f^L - lines) computations for $St = 0.2$: circle/line and $St = 1$: plus symbol/dashed line.

last case, the spray is ejected from the center core and concentrated in weak vorticity areas. It is thus well suited for robustness evaluation of the multi-fluid method. Higher Stokes numbers are not tackled here since it was shown in Reveillon & Demoulin 2007 that, for Stokes number greater than unity, the droplets are inertial enough to be ejected from a vortex and droplet trajectory crossing strongly occurs.

To assess the multi-fluid description of the size-conditioned dynamics, Eulerian multi-fluid density fields are qualitatively compared to Eulerian density fields determined by considering the Lagrangian droplets accumulated around each node, for the same Stokes numbers at the same time set to $t = 0ms$ that has been obtained over tens of eddy turnover times (see figure 2). Both qualitative and quantitative comparisons can be done focusing both on the vacuum zones description and the density level. The repartition of these vacuum zones obtained by the classical Lagrangian method is very precisely reproduced by the EMM. Furthermore, the evolution of droplet repartition with inertia is very well captured by the multi-fluid. Indeed, the Eulerian density fields for higher Stokes number still present a very good agreement with the Lagrangian droplet repartitions (see figure 2).

3.2. Spray evaporation

Once dynamical equilibrium is reached between the turbulent gaseous flow and the dispersed phase, the relative time is set to zero and evaporation is activated. To begin with, there is no chemical reaction, so the evolution of the main characteristics of the vapor mixing can be compared between both formulations. Generally, mixing-based studies refer to the evolution of mean and deviation of the mixture fraction, which is equivalent to the fuel mass fraction in non-reactive cases. The characteristic evaporation delay (at burnt gases temperature) has been set to $\tau_v = 1.26ms$, which corresponds to 1.5 eddy turn over time. Note that when a flame propagates in the domain, the evaporation delay increases because droplets are initially embedded in fresh gases. The time evolution of the mean vapor mass fraction $\langle Y_s^\alpha \rangle$ issued from the evaporation of the spray surrounded by hot gases is plotted in figure 3 (left). The Stokes number (and therefore the preferential segregation) has no effect on the evolution of the mean mass fraction. These results can be expected since the saturation level is temperature based since the mass fraction of vapor remains small. However, there is a small discrepancy in the final mass fraction, a direct consequence of the constant density assumption that implies a local adaptation of the mixture that generates an error up to 5% depending on local spray segregation.

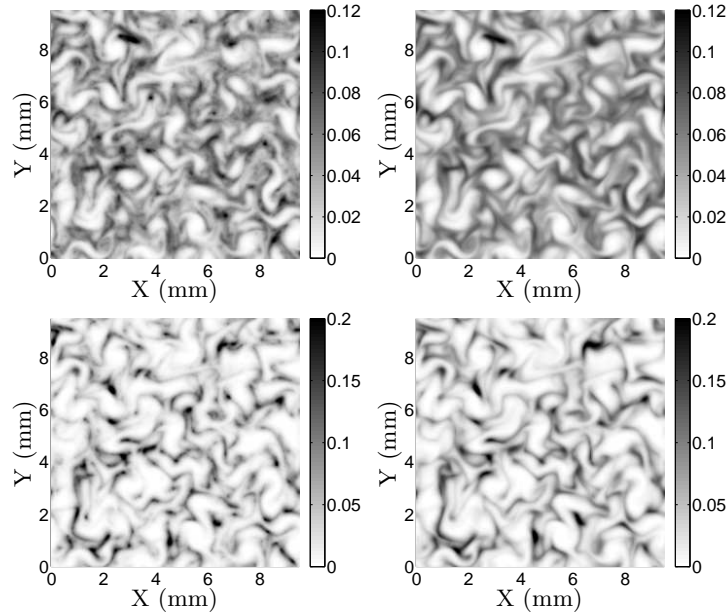


FIGURE 4. Fuel vapor mass fraction obtained from the Lagrangian (Y_f^L - left) and Eulerian (Y_f^E - right) simulations for $St = 0.2$ (top) and $St = 1$ (bottom) at $t = 0.63ms$, which corresponds to half the characteristic evaporation delay.

However, the important point is that both Lagrangian and Eulerian procedures give similar results. The key when modeling turbulent combustion is to capture accurately the mixture fraction variance, which is an inlet parameter of any turbulent combustion model. Now, it is possible to see in figure 3 (right) that the EMM captures properly the fluctuations of the vapor mass fraction, whatever the droplet dynamic is. The strong segregation of case $St = 1$ is reflected in the corresponding level of the mixture fraction root mean square (rms), that can be twice the one of case $St = 0.2$. In the case of reacting flows it can modify deeply the combustion properties. The ability of the EMM to capture these fluctuations is of extreme importance. In figure 4, the fuel vapor mass fraction is obtained from the Lagrangian and the Eulerian simulation for both Stokes after half the characteristic evaporation delay. The fact that a mono-dispersed spray is considered initially underlines the quality of the results. Such an initial Dirac delta function in phase space is one of the most difficult cases to deal with using a multi-fluid model but still leads to very good results. The extension to an initially polydisperse spray would be straightforward and eventually more favorable to the Eulerian multi-fluid model.

3.3. Turbulent spray combustion

To evaluate the EMM in the framework of spray combustion, a second set of analyses has been carried out. In this case, a small core of burnt gases has been embedded in the center of the simulation domain. Since gases are hot, the surrounding droplets vaporize and a flame is then able to propagate. Note that this study is done starting from the relative time $0ms$, when droplets are in dynamical equilibrium with the surrounding gas. The time evolution of the flame front has been plotted in figure 5 for the most difficult case presenting the highest segregation rate ($St = 1$). It is clear that the EMM is able to characterize the spray dispersion and evaporation so that the propagating flame

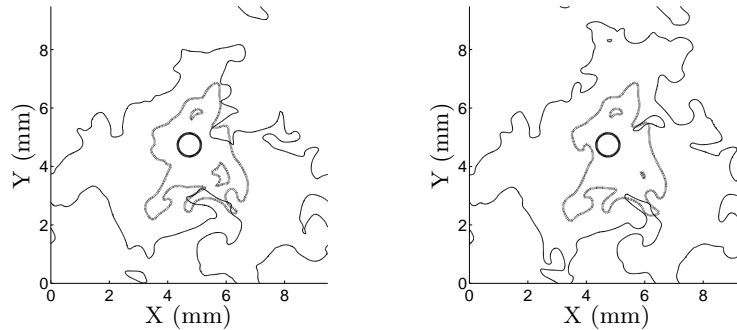


FIGURE 5. Time evolution of the flame fronts obtained from the Lagrangian (left) and the Eulerian (right) simulations. Case $St = 1$, at time $t = 0$ (bold line), $t = 6ms$ (dashed line) and $t = 12ms$ (continuous line).

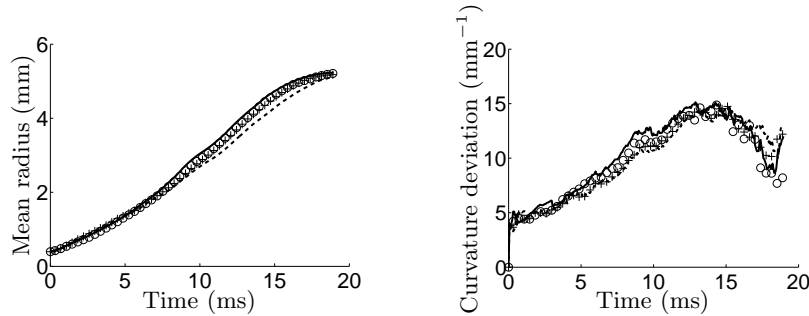


FIGURE 6. Time evolution of flame mean radius (left) and curvature (right). Lagrangian (lines) and Eulerian (symbols) for $St = 0.2$ (line and circles), $St = 1$ (dashed line and plus symbols).

is accurately captured compared to the reference Lagrangian simulation. Note that a similar conclusion may be drawn from the case ($St = 0.2$) that has not been plotted. A quantitative analysis has been carried out in figure 6 on the flame front evolution. In the left figure, the time evolution of the mean flame radius has been plotted. In the Lagrangian simulations, it is possible to observe that the flame propagates faster when droplets are less segregated ($St = 0.2$). Although the difference is slight, it is clearly visible. On the other hand, the EMM presents some difficulties in capturing this difference but the general flame position is correctly captured during the whole time. Another important conclusion may also be drawn from figure 6 (right) since both the Lagrangian model and EMM are able to capture the flame curvature in the whole time. Of course, the flame structure evolution is mainly driven by the surrounding turbulence and the initial segregation of the droplets, but then the flame controls the evaporation rate that is handled by the EMM. Therefore, flame/EMM interactions are captured correctly. It is a very encouraging result considering that it is the first time that the EMM has been applied to a turbulent combustion simulation.

An interesting example of local flame extinction may be seen in figure 7, which focuses on a flame-to-flame interaction. The flame structures are alike, although extinction in the Lagrangian simulation occurs a few microseconds after the one obtained with the EMM. However, as it was shown before, this slight discrepancy does not affect the global flame structure or its major properties (propagation velocity and curvature). In the same figure it is possible to observe the ability of the EMM to capture highly segregated spray areas with droplets following a thin line corresponding to the lowest local vorticity. It

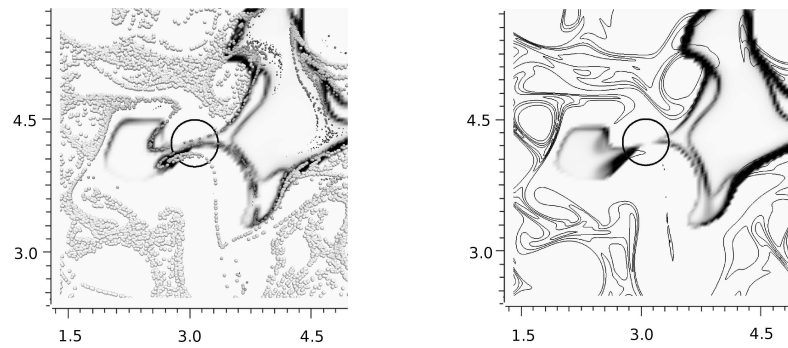


FIGURE 7. Zoom on a flame to flame interaction leading to a local flame extinction. The reaction rate is plotted over Lagrangian droplets (left) and isocontour of Eulerian density (right) for $St = 0.2$, at time $t = 4.67ms$.

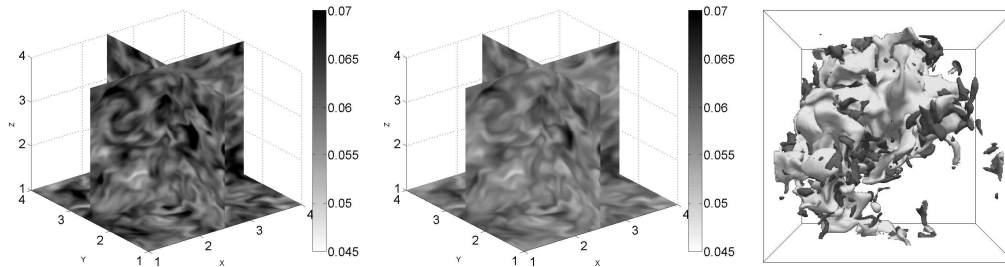


FIGURE 8. Fuel vapor mass fraction obtained from the Lagrangian (Y_f^L - left) and Eulerian (Y_f^E - middle) simulations for $St = 0.2$ at $t = 6.3ms$. Snapshot of an iso-temperature/iso- Y_f (right) showing the development of the flame and evaporation zones with a Eulerian multi-fluid description of the spray at time $t = 12.6ms$.

is also possible to observe that complex flame structures are captured. For example, in the top right of the geometry a double flame front appears corresponding to a first premixed front followed by a diffusion front. Such flames have been analyzed in a purely Lagrangian framework in Reveillon & Vervisch (2005). It is very encouraging, from a turbulent combustion point of view, to note that the EMM can deal with such complex flame structures.

In the 3D configuration, detailed analysis of the fields is still in progress, but comparison of the fuel vapor mass fraction in the purely evaporating case is very well reproduced between the two simulations (figure 8 (left) and (middle)). Furthermore, figure 8 (right) provides a snapshot of a 3D polydisperse spray flame dynamics where the liquid phase is described by a Eulerian multi-fluid model. Thus, numerical simulations of reactive two-phase flows have been carried out in 2D and 3D geometries. A specific coupling between a Lagrangian and a Eulerian multi-fluid formulation has been done to evaluate the ability of the multi-fluid model to characterize properly the major properties of a turbulent reactive flow. It appears that the Eulerian model captured accurately the droplet dispersion and segregation, the vapor turbulent micro-mixing, as well as the flame structures and regimes. As a first step, some simplifying assumptions have been adopted, the most important of which is the use of a constant density flow. However, the intrinsic nature of the EMM is not based on this assumption, and its performance in variable density flows should remain unchanged and will be investigated in future work.

Acknowledgments

The authors wish to thank the Center for Turbulence Research at Stanford University for its hospitality, financial and technical support. This work was granted access to the HPC resources of IDRIS-CINES under the allocations 2010-x2010026172 (M. Massot) and 2010-x2007062032 (J. Reveillon) by GENCI (Grand Equipement National de Calcul Intensif).

REFERENCES

- DE CHAISEMARTIN, S. 2009 *Polydisperse evaporating spray turbulent dispersion: Eulerian model and numerical simulation*. PhD Thesis, Ecole Centrale Paris. Available on TEL : <http://tel.archives-ouvertes.fr/tel-00443982/en/>.
- COSTA, F. 2000 Effects of exothermicity on unsteady diffusion flames. *International Communications in Heat and Mass Transfer* **27** (2), 201–210.
- FRÉRET, L., DE CHAISEMARTIN, S., RÉVEILLON, J., LAURENT, F. & MASSOT, M. 2010 Eulerian models and three-dimensional numerical simulation of polydisperse sprays. In *Proceedings of the International Conference on Multiphase Flows, Tampa, Florida*, pp. 1–12. Available on HAL : <http://hal.archives-ouvertes.fr/hal-00498207/en/>.
- GARCIA, M. 2009 *Développement et validation du formalisme Euler-Lagrange dans un solveur parallèle non-structuré pour la simulation aux grandes échelles*. PhD Thesis, Institut National Polytechnique de Toulouse.
- GOUESBET, G. & BERLEMONT, A. 1998 Eulerian and Lagrangian approaches for predicting the behaviour of discrete particles in turbulent flows. *Progress in Energy and Combustion Science* **25** (2), 133–159.
- GREENBERG, J., MCINTOSH, A. & BRINDLEY, J. 2001 Linear stability analysis of laminar premixed spray flames. *Proc. R. Soc. Lond.* **457**, 1–31.
- GUICHARD, L., REVEILLON, J. & HAUGUEL, R. 2004 Direct numerical simulation of statistically stationary one- and two-phase turbulent combustion: a turbulent injection procedure. *Flow, Turbulence and Combustion* **73**, 133–167.
- KAH, D., LAURENT, F., FRÉRET, L., DE CHAISEMARTIN, S., R.O.FOX, REVEILLON, J. & MASSOT, M. 2010 Eulerian quadrature-based moment models for polydisperse evaporating sprays. *Flow, Turbulence and Combustion* In Press.
- LAURENT, F. & MASSOT, M. 2001 Multi-fluid modeling of laminar poly-dispersed spray flames: origin, assumptions and comparison of the sectional and sampling methods. *Combustion Theory and Modelling* **5**, 537–572.
- LESIEUR, M. 2007 *Turbulence in Fluids. Fluids Mechanics and its Applications* ISBN: 978-1402064340. Springer-Verlag New York Inc.
- MASSOT, M., DE CHAISEMARTIN, S., FRÉRET, L., KAH, D. & LAURENT, F. 2009 Eulerian multi-fluid models: modeling and numerical methods. In *Modelling and Computation of Nanoparticles in Fluid Flows*, pp. 1–86. Lectures of the von Karman Institute. NATO RTO AVT 169. Available on HAL : <http://hal.archives-ouvertes.fr/hal-00423031/en/>.
- REVEILLON, J. & DEMOULIN, F. 2007 Effects of the preferential segregation of droplets on evaporation and turbulent mixing. *Journal of Fluid Mechanics* **583**, 273–302.
- REVEILLON, J. & VERVISCH, L. 2005 Analysis of weakly turbulent dilute-spray flames and spray combustion regimes. *Journal of Fluid Mechanics* **537**, 317–347.